Received: 24 July 2022 | Revised: 16 November 2022 | Accepted: 22 November 2022

DOI: 10.1111/cas.15679

ORIGINAL ARTICLE

Cancer Science WILEY

miR-548ag functions as an oncogene by suppressing MOB1B in the development of obesity-related endometrial cancer

Huai Pang | Jingzhou Wang | Qianqian Wei | Jie Liu | Xiaolong Chu | Chenggang Yuan | Bingqi Yang | Menghuan Li | Dingling Ma | Yihan Tang | Cuizhe Wang | Jun Zhang

Medical College of Shihezi University, Shihezi, China

Correspondence
Cuizhe Wang, Medical College of Shihezi University, Bei-Er-Lu, Shihezi 832000, Xinjiang, China.
Email: wcz905@shzu.edu.cn

Jun Zhang, Shihezi University School of Medicine, Bei-Er-Lu, Shihezi 832000, Xinjiang, China.
Email: zhangjunyc@163.com

Funding information
National Natural Science Foundation of China, Grant/Award Number: 82160496; Projects of Shihezi University, Grant/Award Number: GJHZ201703

Abstract

Obesity is a high-risk factor in the development of endometrial cancer (EC). Our previous study observed that miR-548ag was significantly overexpressed in the sera of obese individuals. Here, we report the function of miR-548ag and its mechanism in promoting the obesity-related progression of EC. The content of miR-548ag was increased in the serum of obese EC individuals. Bioinformatics analysis indicated that the survival rate of EC patients with a higher expression of miR-548ag was significantly reduced. The *Mps One Binder Kinase Activator 1B* (*MOB1B*, the core member of the Hippo signaling pathway) is a direct target gene of miR-548ag, which is inversely correlated with the expression of miR-548ag. The overexpression of miR-548ag enhances the proliferation, invasion, and migration, and inhibits apoptosis by downregulating the expression of MOB1B, leading to the deactivation of the Hippo pathway in EC cell lines and contributing to tumor progression in vivo. Our study has established that miR-548ag functions as an oncogene by suppressing MOB1B in the development of obesity-related EC.

KEYWORDS
endometrial cancer, Hippo pathway, miR-548ag, MOB1B, obesity

1 | INTRODUCTION

Endometrial cancer, also called uterine corpus cancer, is the sixth-most commonly diagnosed cancer in women. The incidence rate of EC is increasing globally, with 417,000 new cases and 97,000 deaths in 2020.[1,2] Although it is more commonly a disease in postmenopausal women, its incidence in younger women of reproductive age is also increasing. Women younger than 40 years comprise up to 5% of EC cases, while ~20% of the cases are diagnosed before menopause. This is partly related to the increasing global trend of obesity, and the observed spurt in disease occurrence in younger women is expected to increase further.[3] An increasing body of evidence indicates that obesity is a high-risk factor in the development of EC.[4–6] However, the mechanism of obesity-related EC is not understood.

Abbreviations: BMI, body mass index; CCND1, cyclin D1; EC, endometrial cancer; FIGO, International Federation of Gynecology and Obstetrics; GLU, glucose; HDL, high-density lipoprotein; IHC, immunohistochemistry; LDL, low-density lipoprotein; MOB1B, Mps One Binder Kinase Activator 1B; NC, normal control; qRT-PCR, quantitative RT-PCR; TBST, TBS-Tween; TC, total cholesterol; TG, triglyceride; XIAP, X-linked inhibitor of apoptosis; YAP1, Yes associated protein 1.

Huai Pang, Jingzhou Wang, and Qianqian Wei contributed equally to this work.

Recently, with the discovery of certain adipose factors, adipose tissue is no longer a simple energy-storage organ but an organ with endocrine functions. Previous studies have demonstrated that adipose tissue is the main repository of circulating exosome-derived microRNAs in vivo.[7] By acting on the 3′UTR region of the target gene, microRNA degrades the target gene mRNA or inhibits its translation, regulates the expression of various oncogenes and tumor suppressor genes at the post-transcriptional level, and thus plays a role in tumor suppression or cancer promotion.[8–10] Therefore, identifying microRNAs that are differentially expressed in vivo after obesity, and elucidating their possible molecular mechanisms, will provide a theoretical basis for the prevention and treatment of EC.

Our study observed that the content of miR-548ag in the sera of obese individuals was markedly increasing. Further analysis of the available databases revealed that the survival rate of patients was significantly reduced due to the elevation of miR-548ag. Bioinformatics, combined with a dual-luciferase reporter assay, confirmed that MOB1B was the downstream target gene of miR-548ag and that the survival rate of EC patients with high expression of MOB1B was significantly increased. In the in vitro experiments using cultured EC cells Ishikawa and HEC-1-A, miR-548ag was confirmed to inhibit the Hippo signaling pathway by downregulating MOB1B, promoting proliferation, invasion, and migration of tumor cells, and inhibiting apoptosis. In the in vivo experiments, it was observed that a high-fat diet could promote the expression of miR-548ag, inhibit the expression of MOB1B, and enhance the tumor-forming ability of Ishikawa cells in nude mice. Moreover, under a normal diet, the tumorigenicity of Ishikawa cells with overexpression of miR-548ag was enhanced in nude mice. Our findings provide novel insights into the role of miR-548ag in the progression of aggressive obesity-related EC.

2 | MATERIALS AND METHODS

2.1 | Collection of serum and tissue specimens

We collected serum and endometrial tissue samples from EC patients ($n = 40$) and non-cancer individuals ($n = 40$) from September 2017 to December 2020 at the First Affiliated Hospital of Shihezi University School of Medicine and Shihezi People's Hospital. All carcinomas and non-carcinomas were classified based on the pathology reports. No radiotherapy or chemotherapy was conducted before surgery and the patients or their relatives signed informed consents. Exclusion criteria for non-cancer individuals: individuals with various types of tumors and malignant wasting diseases. This study was approved by the First Affiliated Hospital of Shihezi University School Ethics Committee (approval number: 2017-050-01).

2.2 | Cell culture and transfection

The human EC cell line Ishikawa (RRID: CVCL_2529) and human embryonic kidney 293T (HEK 293T, RRID: CVCL_0063) were obtained from Procell and maintained in DMEM containing 10% FBS and 1% penicillin and streptomycin at 37°C in a humidified atmosphere containing 5% CO_2. The human EC cell line HEC-1-A (RRID: CVCL_0293) was obtained from the National Collection of Authenticated Cell Culture and maintained in McCoy's 5A medium containing 10% FBS and 1% penicillin and streptomycin at 37°C in a humidified atmosphere containing 5% CO_2. All cell lines have been authenticated using short tandem repeat profiling within the last 3 years and tested for mycoplasma contamination by DAPI staining. All experiments were performed with mycoplasma-free cells. The cells were transfected with a miR-548ag mimic, miR-548ag inhibitor, and MOB1B-overexpression plasmid, using the Lipofectamine 2000 reagent according to the manufacturer's instructions. The miR-548ag mimic and miR-548ag inhibitor were constructed by Genepharm. The MOB1B-overexpression plasmid was constructed by SyngenTech.

2.3 | RNA extraction and quantitative real-time polymerase chain reaction

Total RNA was extracted from cells and tissues using TRIzol reagent (Invitrogen), according to the manufacturer's instructions. miRNA was extracted from the serum using the miRcute serum/plasma miRNA isolation kit (TIANGEN), according to the manufacturer's protocol. U6 and GAPDH were used as endogenous controls to normalize miRNA and mRNA, respectively. mRNA and miRNA were then reverse transcribed to complementary DNA (cDNA) using the Revert Aid First-Strand cDNA kit (Thermo Scientific) and miRNA First-Strand cDNA kit (TIANGEN), respectively, according to the manufacturer's protocols. qRT-PCR was performed in triplicate on the Rotor-Gene Q MDx detection system (QIAGEN) using the SYBR Green PCR kit (QIAGEN) and miRNA qPCR kit (TIANGEN) to detect mRNA and miRNA, respectively. Relative changes in the expression levels of the mRNA and miRNA were quantified using the $2^{-\Delta\Delta CT}$ method. All primers used in our study were as follows: MOB1B forward, 5′-TTCGGATGGCT GTCATGCTTCC-3′, reverse, 5′-GCTGACA TCACTGGACAACTCTC-3′; CCND1 forward, 5′-TCTACACCGACAACTCCATCCG-3′, reverse, 5′-TCTGGCATTTTGG AGAGGAAGTG-3′; XIAP forward, 5′-TGGCAGATTATGAAGCA CGGATC-3′, reverse, 5′-AGTTAGCCCTCCTCCACAGTGA-3′; GAPDH forward, 5′-GGTGGTC TCCTCTGACTTCAA-3′, reverse, 5′-TCTTCC TCTTGTGCTCTTGCT-3′.

2.4 | Immunohistochemistry

All samples were fixed in 4% formaldehyde solution and embedded in paraffin. Then, paraffin-embedded sections were dewaxed in xylene and rehydrated in graded alcohol. The sections were sequentially incubated with anti-MOB1B rabbit polyclonal antibodies (ap7031b), anti-CCND1 rabbit monoclonal antibodies (ab16663), and anti-XIAP rabbit polyclonal antibodies (ab21278) at dilutions of 1:1000, overnight at 4°C. Then, the sections were incubated with HRP-conjugated

anti-rabbit antibodies for 30 min at 37°C. Subsequently, two experienced teachers in the pathology department were invited to perform IHC scores for the tissue sections. Scoring was based on the percentage of positive cells: 0%–5%—0 points, 6%–25%—1 point, 26%–50%—2 points, 51%–75%—3 points, 76%–100%—4 points; positive intensity: negative—0 point, light brown—1 point, claybank—2 points, brown—3 points. Total score = percentage score of positive cell number × positive intensity score.

2.5 | Western blotting

The cells and tissues were lysed in ice-cold RIPA lysis buffer according to the manufacturer's instructions. The concentration of proteins was determined by bicinchoninic acid (BCA) assay. Then, the proteins were resolved by 10% SDS-PAGE and transferred onto PVDF membranes. After blocking with 5% BSA for 3 h, the membranes were incubated with anti-β-actin mouse monoclonal antibodies (TA-08), anti-MOB1B rabbit polyclonal antibodies (ap7031b), anti-CCND1 rabbit monoclonal antibodies (ab16663), and anti-XIAP rabbit polyclonal antibodies (ab21278) at a 1:1000 dilution overnight at 4°C. Then, the membranes were incubated with HRP-conjugated anti-rabbit antibodies for 2 h after washing three times with TBST buffer. Finally, the membranes were flooded with an Enhanced Chemiluminescence Detection reagent and detected using a chemiluminescence analyzer.

2.6 | Cell proliferation assay

Cell proliferation was measured using the CCK-8 reagent (DOJINDO). First, the cells were seeded into 96-well plates (5×10^3 cells/well) and cultured in a complete medium for 24 h. Then, cell proliferation was assessed every 24 h (up to 72 h) after transfection with the miR-548ag mimic, miR-548ag inhibitor, and MOB1B-overexpression plasmid. Finally, 10 μl of the CCK-8 solution was added to the medium in each well, and incubated for 2 h, and the absorbance values were then measured at 450 nm using a full-wavelength microplate reader (Thermo).

2.7 | Colony formation assay

The cells were seeded into six-well plates (500 cells/well) and cultured in DMEM for 2 weeks after transfection with the miR-548ag mimic, miR-548ag inhibitor, and MOB1B-overexpression plasmid. The colonies were stained with 0.1% crystal violet after fixing with a 4% fixative solution (Solarbio).

2.8 | In vitro cell invasion and migration assay

To evaluate the migratory and invasive abilities of the EC cells, 24-well Transwell Permeable Support plates (Corning) were used. First, the cells that were transfected with the miR-548ag mimic, miR-548ag inhibitor, and MOB1B-overexpression plasmid were collected after 24 h. Then, cells at a concentration of 1×10^5/well were resuspended in 200 μl of serum-free medium and seeded into the upper chamber containing an uncoated or Matrigel-coated membrane, and then a medium containing 20% FBS (600 μl) was added to the lower chamber. Finally, the cells that invaded or migrated to the lower membrane were fixed in a 4% fixative solution and stained with 0.1% crystal violet after incubation for 24 h at 37°C in a humidified 5% CO_2 incubator. The numbers of invading and migrating cells were counted in nine high-powered (×200) fields under a light microscope.

2.9 | Wound-healing assay

EC cells in the exponential growth stage were digested with trypsin and inoculated into six-well plates. At 24 h after transfection, linear wounds were created in the confluent monolayers using a pipette tip and the shed cells were washed three times with sterile PBS buffer. Then, at 0, 24, and 48 h, images were captured using a light microscope to compare the migration ability.

TABLE 1 Clinical features of benign lesions and endometrial cancer

	Benign lesions	Endometrial cancer
n	30	30
BMI, kg/m^2, *n* (%)		
<24	20 (67)	4 (13)
24–28	8 (27)	10 (33)
>28	2 (6)	16 (54)
Mean (range)	23.63 (18.66–28.28)	28.22 (19.78–43.66)***
Biochemical index, mean (range)		
TC	4.44 (3.30–5.69)	5.34 (3.12–7.80)***
TG	1.44 (0.47–4.88)	1.89 (0.74–5.91)*
HDL	1.28 (0.79–2.34)	1.25 (0.83–1.74)
LDL	2.46 (0.25–4.05)	3.23 (0.92–5.45)**
GLU	4.85 (4.13–6.17)	7.09 (4.52–14.82)***
FIGO stage, *n* (%)		
I/II	0 (0)	27 (90)
III/IV	0 (0)	3 (10)
Grade, *n* (%)		
1	0 (0)	13 (43)
2	0 (0)	17 (57)
3	0 (0)	0 (0)
Lymphatic metastasis, *n* (%)		
+	0 (0)	0 (0)
−	30 (100)	30 (100)

Note: *T*-test, Mann–Whitney *U*-test.
*$p<0.05$, **$p<0.01$, ***$p<0.001$.

2.10 | Apoptosis assay

Cell apoptosis was detected using the Annexin V-FITC/PI apoptosis kit (Multi Sciences) according to the manufacturer's protocol, and flow cytometry. Attention was paid to the reduction in cellular mechanical damage during cell treatment.

2.11 | Dual-luciferase reporter assay

The 3′UTR sequences of the MOB1B-containing mutant (MUT) or wild-type (WT) miR-548ag-binding sites were constructed by Genepharm and cloned into a GP-miRGLO luciferase reporter vector. The HEK 293T cells were seeded into 96-well plates and co-transfected with either the WT-MOB1B or the MUT-MOB1B 3′UTR reporter plasmids along with the miR-548ag mimic or normal control (NC). Firefly and Renilla luciferase activities were assessed using the Dual-Luciferase Assay System (Promega), according to the manufacturer's protocol. The relative expression of the firefly luciferase activity was normalized to the Renilla luciferase activity.

2.12 | Animal experiments

In this study, all animal experiments were approved by the First Affiliated Hospital of Shihezi University School Ethics Committee (approval number: A2021-022-01). Four-week-old female BALB/C nude mice were purchased from HUNAN SJA Animal Laboratory, Co., Ltd. After 1 week of adaptive feeding, animals were divided randomly into the normal-diet (ND) group ($n = 15$) and the high-fat diet (HFD) group ($n = 5$). After 4 weeks of feeding, the obesity model was successfully constructed (the weight of nude mice in the HFD group was 20% higher than that in the ND group). Then, 3×10^6 Ishikawa cells with stable overexpression of the miR-548ag NC ($n = 5$) and Ishikawa cells with stable overexpression of miR-548ag ($n = 5$) were subcutaneously injected into nude mice in the ND group, whereas, mice in the HFD group were subcutaneously injected with 3×10^6 Ishikawa cells ($n = 5$). The weights and tumor volumes of the mice were determined every 3 days. Tumor volume was assessed by measuring the length (L) and width (W) of the tumor using calipers (tumor volume, $mm^3 = 0.5 \times L \times W^2$). After 6 weeks, the mice were euthanized and the tumors were excised, measured, and photographed.

2.13 | Bioinformatics analysis

Bioinformatics software TargetScan[11] and miRDB[12] were used to predict the downstream target genes and targeted binding sites of miR-548ag. Kaplan–Meier Plotter[13] and OncoLnc database[14] were used to analyze the relationship between the expression levels of miR-548ag and MOB1B and the survival rate of EC patients. The StarBase database[15] was used to analyze the expression of MOB1B, CCND1, and XIAP in EC.

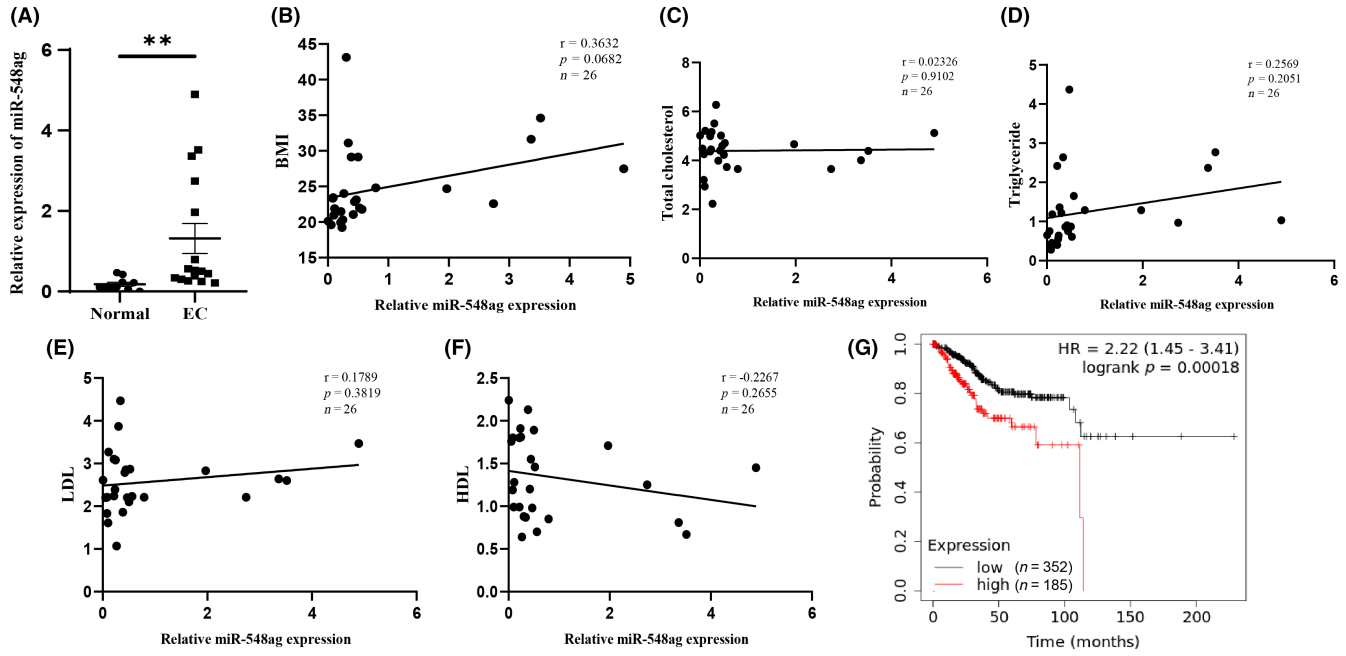

FIGURE 1 Analysis of the correlation of the expression level of miR-548ag with obesity-related indicators and the prognosis of subjects. (A) Expression levels of miR-548ag were detected in the sera of normal ($n = 10$) and endometrial cancer (EC) ($n = 16$) patients. (B–F) Correlation between the expression levels of miR-548ag in the sera of subjects and obesity-related indicators (body mass index [BMI]/total cholesterol [TC]/triglyceride [TG]/low-density lipoprotein [LDL]/high-density lipoprotein [HDL]). (G) Relationship between the expression level of miR-548ag and patient survival rate; T-test, $^{**}p < 0.01$.

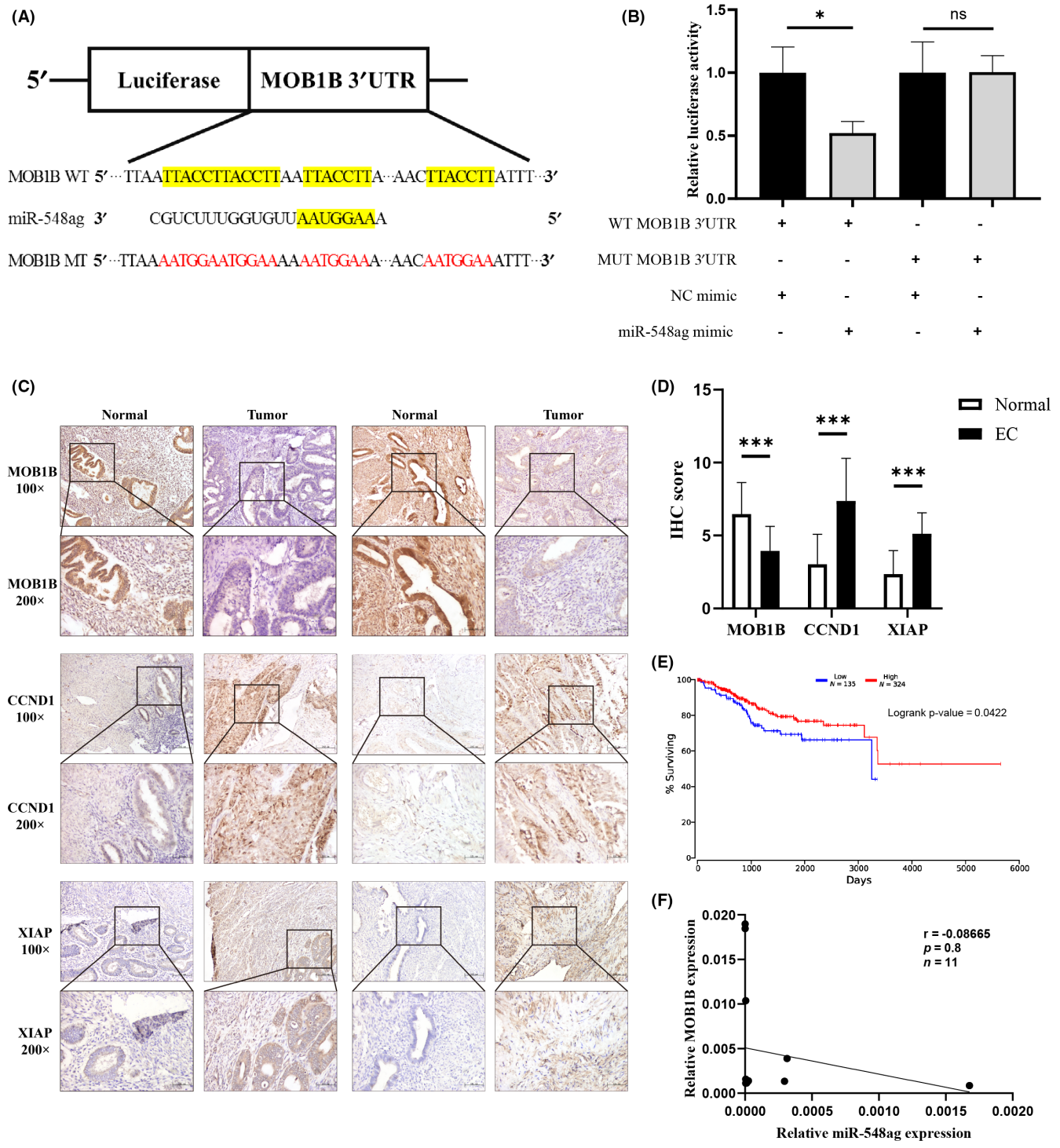

FIGURE 2 MOB1B is the target gene of miR-548ag, which is significantly underexpressed in endometrial cancer (EC) and positively correlated with prognosis. (A) The putative miR-548ag binding sites and mutations at the sites in MOB1B predicted by TargetScan database. (B) Analysis of the activity of the double luciferase reporter gene plasmid in HEK 293T cells. (C) Expression levels of MOB1B, CCND1, and XIAP were detected by immunohistochemistry (IHC) in normal ($n = 30$) and EC ($n = 34$) under ×100 and ×200 mirrors. (D) IHC score. (E) Relationship between the expression level of MOB1B and the survival rate of patients. (F) Correlation between miR-548ag and the expression level of MOB1B; *T*-test, Mann–Whitney *U*-test, $^{*}p < 0.05$, $^{***}p < 0.001$.

2.14 | Immunofluorescence assay

Cells grown on 24-well plates were fixed in 4% paraformaldehyde for 20 min at 4°C and permeabilized with 0.5% Triton-X-100 for 20 min. Then cells were blocked with 5% BSA for 30 min at room temperature, followed by incubation with anti-YAP1 primary antibodies (ab205270) at a 1:500 dilution overnight at 4°C. The next day, 24-well plates were rewarmed in an oven at 37°C for 30 min. Then,

Alexa Fluor-conjugated secondary antibodies (ab150077) according to 1:1000 dilution were incubated for 1 h at 37°C. Cell nuclei were stained with DAPI in the dark for 5 min. Finally images were analyzed using a fluorescence microscope.

2.15 | Statistical analysis

All data were presented as the mean ± SD of at least three independent experiments. The statistical software SPSS version 17.0 was used for data analysis. Student's *t*-test was used to compare the mean values of normally distributed data between groups, while the Mann–Whitney *U*-test was used for non-normally distributed data. A *p*-value of <0.05 indicated statistically significant differences between the groups.

3 | RESULTS

3.1 | miR-548ag is upregulated in obesity-related EC and is associated with reduced overall survival

It was observed that BMI, total cholesterol, triglyceride, LDL, and fasting blood glucose were significantly increased in EC patients compared with non-cancer individuals ($p < 0.05$) (Table 1). The content of miR-548ag in the sera of EC patients was significantly higher than in non-cancer individuals ($p < 0.05$) (Figure 1A), and was positively correlated with BMI, total cholesterol, triglyceride, and LDL of the subjects and negatively correlated with HDL ($p > 0.05$) (Figure 1B–F). Moreover, analysis of the Kaplan–Meier survival curve indicated that EC patients with a high expression of miR-548ag showed a significantly shorter survival time than those with a lower expression of miR-548ag ($p < 0.05$) (Figure 1G).

3.2 | MOB1B is a direct target of miR-548ag and is inversely correlated with the expression of miR-548ag

First, we used the bioinformatics-based miRNA target-prediction programs TargetScan and miRanda to identify potential miR-548ag target genes. MOB1B was selected as a candidate as it had a latent miR-548ag-binding site in its 3′UTR. The WT and mutant-type (MT) dual-luciferase reporter plasmid of MOB1B 3′UTR were constructed based on the predicted binding sites (Figure 2A). The dual-luciferase reporter assay results in HEK 293T cells indicated that co-transfection with the miR-548ag mimic and MOB1B-WT 3′UTR led to declined luciferase activity compared with that in the control group (MOB1B-MT 3′UTR) ($p < 0.05$) (Figure 2B).

Subsequently, the IHC results indicated that the protein expression levels of MOB1B in EC tumor tissues were significantly decreased compared with the endometrial tissues of non-cancerous individuals, whereas the protein expression levels of CCND1 and XIAP were significantly increased ($p < 0.05$) (Figure 2C,D). Moreover, analysis of the OncoLnc database revealed that the survival rate of patients with low expression of MOB1B decreased significantly ($p < 0.05$) (Figure 2E). In endometrial tissues, the expression level of miR-548ag was negatively correlated with that of MOB1B ($p > 0.05$) (Figure 2F).

3.3 | miR-548ag enhances the proliferation, invasion, and migration, as well as inhibits apoptosis by deactivating the Hippo pathway in EC cell lines

To further understand the role of miR-548ag in the development of EC and its possible molecular mechanisms, we first overexpressed miR-548ag by transfecting its mimic and downregulated miR-548ag by transfecting its inhibitor in EC cells. qRT-PCR and western blot analysis indicated that the overexpression of miR-548ag inhibited the expression of MOB1B and increased the expression of the Hippo pathway downstream factors CCND1 and XIAP, as well as increased the nuclear entry of YAP1 and decreased the expression of phosphorylated YAP1. In contrast, downregulation of the expression of miR-548ag showed the opposite effect ($p < 0.05$) (Figure 3A–D; Figures S1A–D and S2).

Then, the CCK-8 assay and the colony formation assay were used to further evaluate the effect of miR-548ag on the proliferation of EC cells. The results indicated that the overexpression of miR-548ag significantly promoted cell proliferation, whereas the downregulation of miR-548ag showed the opposite effect ($p < 0.05$) (Figure 3E–G; Figure S1E,F). The Transwell assay and wound-healing assay demonstrated that the overexpression of miR-548ag exerted an active effect on the invasion and migration of EC cells, whereas the

FIGURE 3 miR-548ag enhances proliferation, invasion, and migration, and inhibits apoptosis of EC cells by deactivating the Hippo pathway. (A–C) Relative expression of MOB1B, CCND1, and XIAP after transfection with the NC mimic, miR-548ag mimic, NC inhibitor, and miR-548ag inhibitor, as determined by qRT-PCR and western blot. (D) Immunofluorescence assay of YAP1 (green) in Ishikawa cell lines after transfection with the NC mimic, miR-548ag mimic, NC inhibitor, and miR-548ag inhibitor. Nuclear staining with DAPI (blue). (E–G) CCK-8, and colony formation assay were used to observe the proliferation of EC cells after transfection with the NC mimic, miR-548ag mimic, NC inhibitor, and miR-548ag inhibitor. (H, I) Effects of alteration in the expression of miR-548ag on the invasion and migration of EC cells using the Transwell assay. (J, K) Numbers of invading and migrating cells were counted in the Transwell assay. (L) Wound-healing assay was used to determine the migration of Ishikawa cells after transfection with the NC mimic, miR-548ag mimic, NC inhibitor, and miR-548ag inhibitor. (M) Effects of alteration in the expression of miR-548ag on apoptosis were detected by flow cytometry. *T*-test, $^{*}p < 0.05$, $^{**}p < 0.01$, $^{***}p < 0.001$.

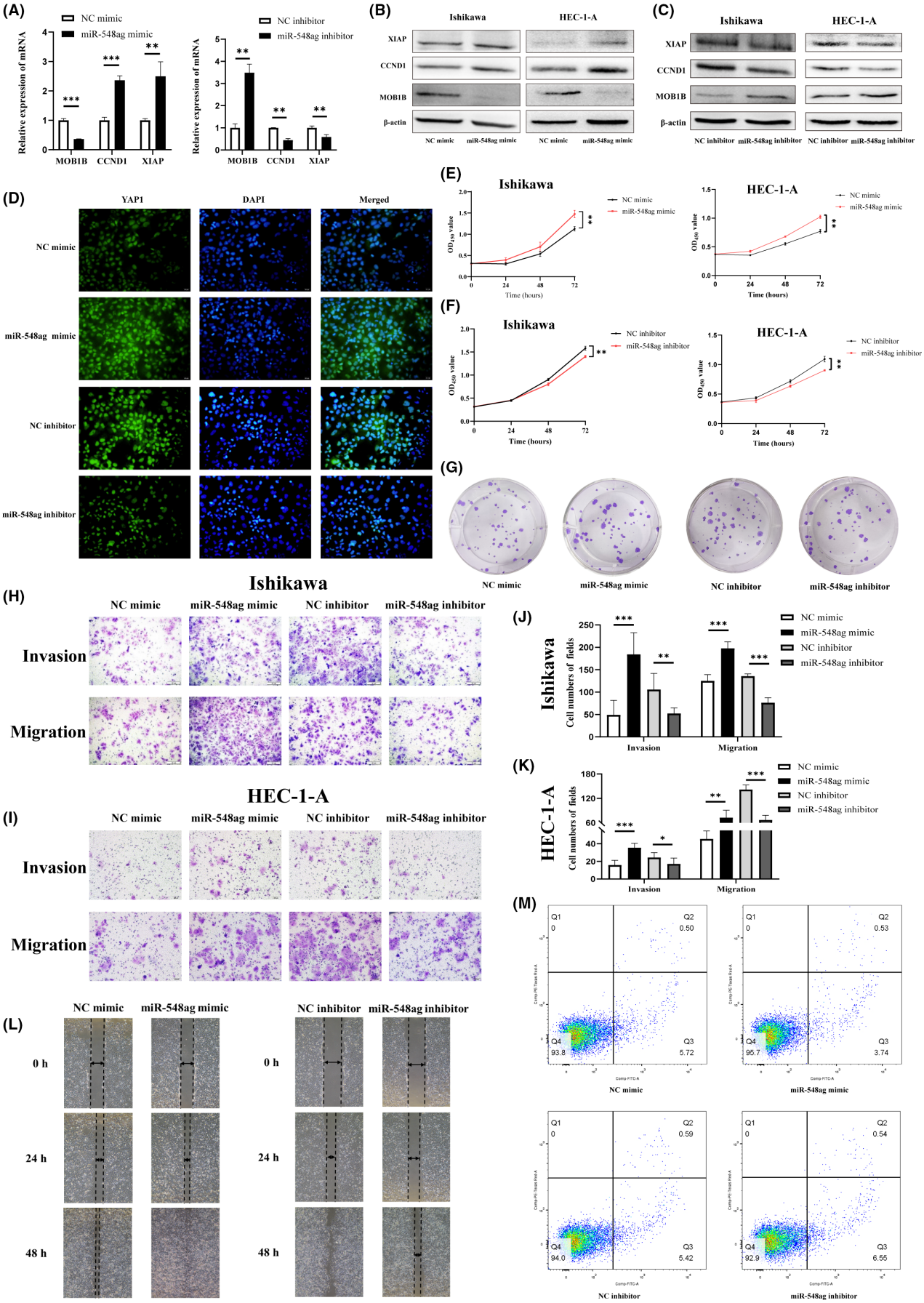
(A)
NC mimic
miR-548ag mimic
Relative expression of mRNA
MOB1B
CCND1
XIAP
NC inhibitor
miR-548ag inhibitor
(B)
Ishikawa
HEC-1-A
XIAP
CCND1
MOB1B
β-actin
NC mimic
miR-548ag mimic
(C)
Ishikawa
HEC-1-A
XIAP
CCND1
MOB1B
β-actin
NC inhibitor
miR-548ag inhibitor
(D)
YAP1
DAPI
Merged
NC mimic
miR-548ag mimic
NC inhibitor
miR-548ag inhibitor
(E)
Ishikawa
HEC-1-A
NC mimic
miR-548ag mimic
OD450 value
Time (hours)
(F)
Ishikawa
HEC-1-A
NC inhibitor
miR-548ag inhibitor
OD450 value
Time (hours)
(G)
NC mimic
miR-548ag mimic
NC inhibitor
miR-548ag inhibitor
(H)
Ishikawa
NC mimic
miR-548ag mimic
NC inhibitor
miR-548ag inhibitor
Invasion
Migration
(I)
HEC-1-A
NC mimic
miR-548ag mimic
NC inhibitor
miR-548ag inhibitor
Invasion
Migration
(J)
Ishikawa
Cell numbers of fields
NC mimic
miR-548ag mimic
NC inhibitor
miR-548ag inhibitor
Invasion
Migration
(K)
HEC-1-A
Cell numbers of fields
NC mimic
miR-548ag mimic
NC inhibitor
miR-548ag inhibitor
Invasion
Migration
(L)
NC mimic
miR-548ag mimic
NC inhibitor
miR-548ag inhibitor
0 h
24 h
48 h
(M)
NC mimic
miR-548ag mimic
NC inhibitor
miR-548ag inhibitor
Q1
Q2
Q3
Q4
0
0.50
5.72
93.8
0.53
3.74
95.7
0.59
5.42
94.0
0.54
6.55
92.9

downregulation of miR-548ag showed the opposite effect ($p < 0.05$) (Figure 3H–L). Furthermore, flow cytometry revealed that the overexpression of miR-548ag reduced cell apoptosis, whereas the downregulation of miR-548ag showed the opposite effect (Figure 3M and Figure S1G,H). These data indicated that miR-548ag enhanced the proliferation, invasion, and migration of EC cells while inhibiting their apoptosis.

3.4 | MOB1B reverses the effects of miR-548ag on endometrial cancer cells

To further verify the pro-carcinogenic effects of miR-548ag by inhibiting the expression of MOB1B, we co-transfected the miR-548ag mimic and MOB1B-overexpressing plasmid in EC cells. The results of qRT-PCR and western blot assay indicated that the expression of MOB1B was significantly reduced, whereas that of CCND1 and XIAP was significantly increased when the miR-548ag mimic was transfected in EC cells. Conversely, co-transfection of the miR-548ag mimic and MOB1B-overexpression plasmid in EC cells significantly reversed the oncogenic effect of miR-548ag ($p < 0.05$) (Figure 4A,B). The immunofluorescence assay revealed that the nuclear entry of YAP1 was increased when the cells were transfected with the miR-548ag mimic and reduced when the cells were co-transfected with the miR-548ag mimic and MOB1B-overexpression plasmid (Figure 4C). Moreover, the simultaneous upregulation of miR-548ag and MOB1B significantly reversed the promoting effects of the upregulation of miR-548ag alone on the migration, invasion, and proliferation of EC cells ($p < 0.05$) (Figure 4D–G). These results confirmed that miR-548ag enhanced the EC process by directly targeting MOB1B in vitro.

3.5 | miR-548ag contributes to the progression of tumors in vivo

We performed xenograft assays to further validate the role of miR-548ag on tumor progression. First, we constructed an obese animal model to observe the effect of obesity on EC cell Ishikawa tumorigenesis. BALB/C nude mice were divided into an HFD group ($n = 5$) and an ND group ($n = 5$). After 4 weeks of feeding, the body weights of the nude mice in the HFD group increased significantly compared with the ND group. Ishikawa cells were subcutaneously injected into nude mice ($p < 0.05$) (Figure 5A,C). After continued feeding until the 10th week, the body weight, average visceral fat weight, TC, and TG levels of the nude mice in the HFD group were significantly higher than those in the ND group ($p < 0.05$) (Figure 5B–E), whereas the volume and weight of the tumor tissue were significantly increased ($p < 0.05$) (Figure 5F–H). Furthermore, the qRT-PCR assay of the tumors in mice indicated significant upregulation of the expression of miR-548ag ($p < 0.05$) (Figure 5I). The western blot assay demonstrated a significant downregulation of the expression of MOB1B and an upregulation of the expression of CCND1 in the HFD group (Figure 5J). The purpose of this part of the experiment was to clarify the relationship between obesity, miR-548ag, and the tumorigenic ability of EC cells in vivo.

Second, we wanted to further observe the effect of miR-548ag on EC cell Ishikawa tumorigenesis. After 4 weeks of a normal diet, the nude mice were divided into an NC group (subcutaneous injection of Ishikawa with miR-548ag NC, $n = 5$) and an miR-548ag group (subcutaneous injection of Ishikawa with stable overexpression miR-548ag, $n = 5$) (Figure 5A). We found that, compared with the NC group, the volume and weight of the tumor tissue of the miR-548ag group showed a significant increase ($p < 0.05$) (Figure 5F–H). Moreover, the expression level of miR-548ag in tumor tissues was significantly increased, as determined by qRT-PCR assay ($p < 0.05$) (Figure 5K), that of MOB1B was significantly decreased, and CCND1 was significantly increased, as determined by western blot assay (Figure 5L). The purpose of this part of the experiment was to focus on the role of miR-548ag. Collectively, these results demonstrated that an HFD could promote the expression of miR-548ag, and that overexpression of miR-548ag inhibited the expression of MOB1B, and enhanced the tumor-forming ability of EC cells in vivo.

4 | DISCUSSION

Although EC is a common disease in postmenopausal women, its incidence in young women of childbearing age has also been increasing in recent years, which is partly related to the globally increasing prevalence of obesity.[3,16,17] The occurrence of type I EC is closely related to obesity and is the most common histological type of EC, accounting for ~85% of all cases.[18–20] Our study showed that the BMI, TC, TG, LDL, GLU, and other obesity-related signs were significantly higher in EC patients compared with non-cancer individuals, further confirming that obesity is an important risk factor in the development of EC. However, the specific molecular mechanisms of the development of EC induced by obesity have not been fully elucidated.

The existing literature demonstrates that miRNA plays an important role in the occurrence and development of obesity-related tumors.[21] However, only a few studies have investigated the relationship between changes in the expression level of miRNA and the occurrence and development of EC after obesity. Our previous research has screened an miRNA called miR-548ag, which is significantly related to the signs of obesity, as well as metabolic and biochemical indicators of the subjects in the population. However, the molecular role of miR-548ag has not been described in the literature. In this study, we observed that the content of miR-548ag in the serum of EC individuals increased significantly, whereas further analysis of the database revealed that the survival rate of the patients was significantly reduced due to elevated miR-548ag. These results indicated that miR-548ag may function as an "oncomir" in EC.

Previous studies have demonstrated that MOB1 plays a key molecular switch role in the Hippo pathway, and its elevated expression can inhibit the occurrence and development of various tumors. A study by Fan reported that the effects of PTEN-induced putative kinase 1-dependent mitophagy causing an inhibition of

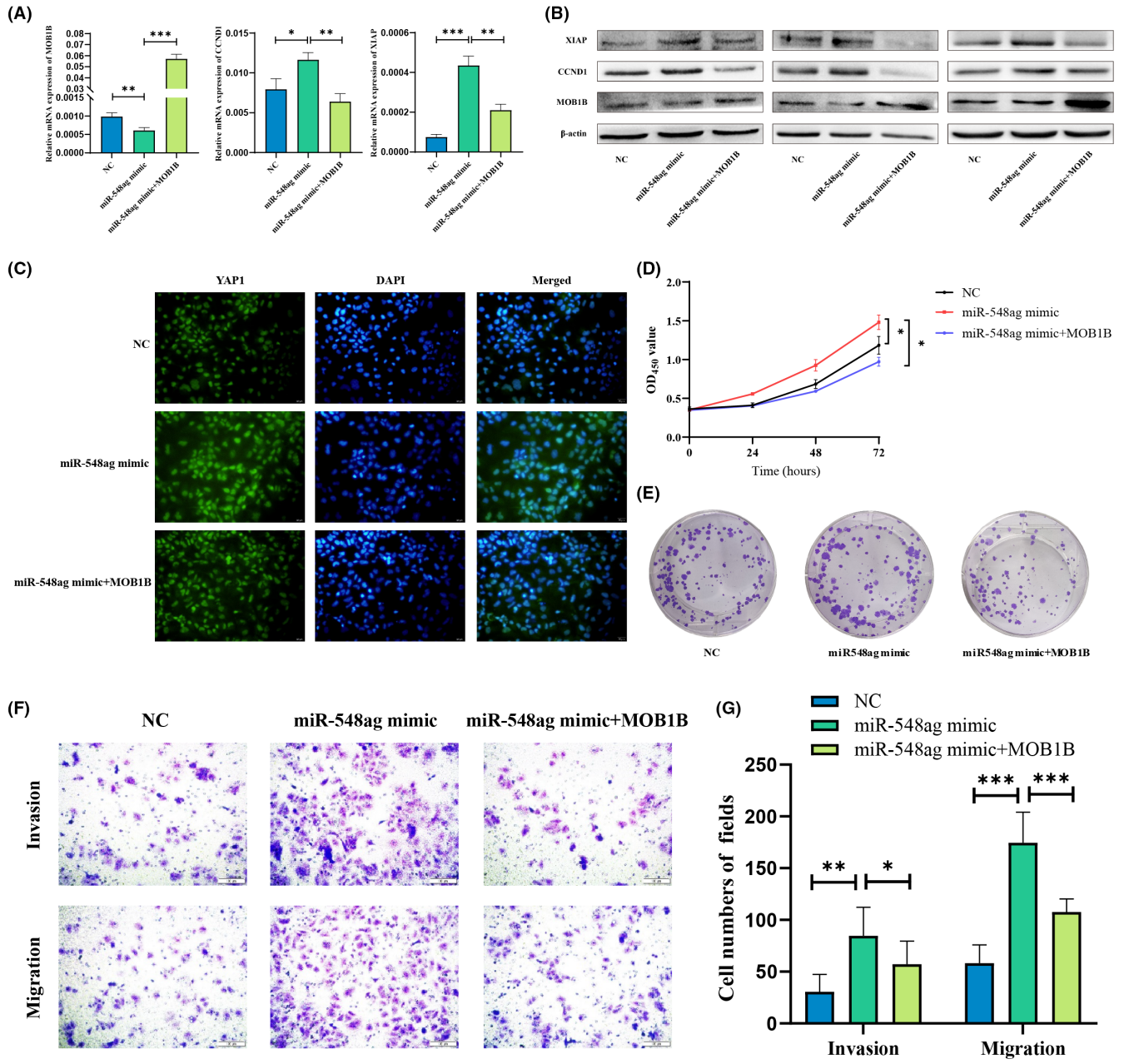

FIGURE 4 MOB1B reverses the effects of miR-548ag on endometrial cancer (EC) cells. (A, B) mRNA and protein expression levels of MOB1B/CCND1/XIAP were detected after transfection of the Ishikawa cells with the NC, miR-548ag mimic, and miR-548ag mimic + MOB1B. (C) Immunofluorescence assay of YAP1 (green) in Ishikawa cells after co-transfection. Nuclear staining was carried out with DAPI (blue). (D, E) CCK-8, and colony formation assay were used to detect the proliferation of Ishikawa cells after co-transfection. (F) Effects of co-transfection on the invasion and migration of Ishikawa cells using the Transwell assay. (G) Numbers of invading and migrating cells were counted in the Transwell assay. *T*-test, $^{*}p < 0.05$, $^{**}p < 0.01$, $^{***}p < 0.001$.

the migration and homing of myeloma cells to calvarium are driven by the activation of the MOB1B-mediated Hippo pathway.[22] Nishio reported that the livers of MOB1A/1 B-specific knockout mice could mediate hepatocarcinogenesis by inhibiting the YAP1/TAZ and TGF-β signaling pathways.[23] Quan reported that lysine demethylase 2 promoted the proliferation, migration, and invasion of pancreatic ductal adenocarcinoma by directly bonding with the promoter region of MOB1 and transcriptionally inhibiting the expression of MOB1.[24] However, the molecular role of MOB1B in EC has not been reported. The study of the database revealed that the survival rate of patients was significantly reduced due to the downregulation of MOB1B.

The target gene prediction software used in this study identified an miR-548ag binding site in the 3′UTR of *MOB1B*, whereas the dual-luciferase reporter assays confirmed that *MOB1B* was a direct target of miR-548ag. To confirm this functional interaction, the overexpression of miR-548ag reduced the expression of both MOB1B mRNA and protein in EC cell lines. Moreover, the

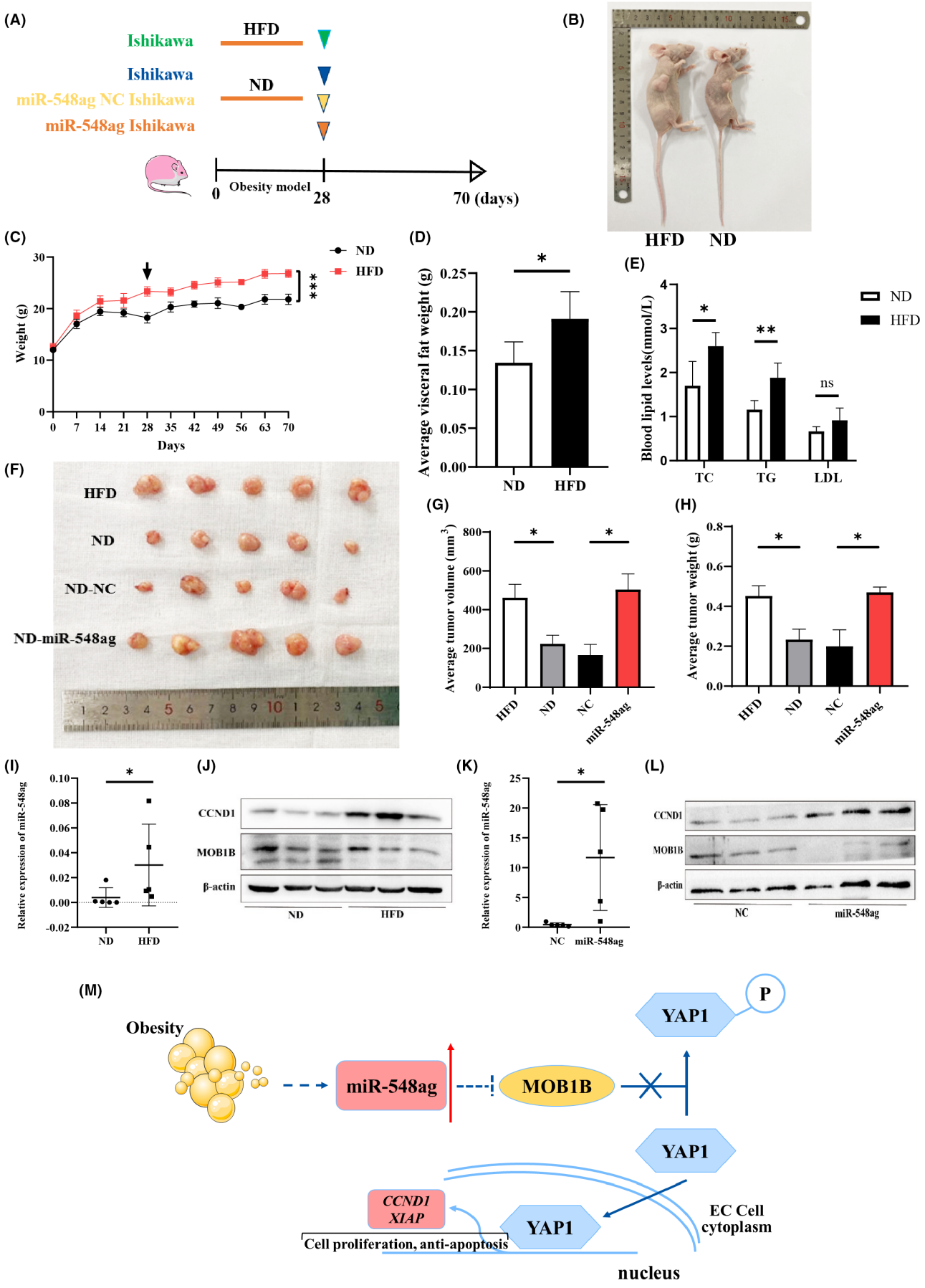
(A)
Ishikawa
HFD
Ishikawa
ND
miR-548ag NC Ishikawa
miR-548ag Ishikawa
0
Obesity model
28
70 (days)
(B)
HFD
ND
(C)
ND
HFD
Weight (g)
Days
(D)
Average visceral fat weight (g)
ND
HFD
(E)
Blood lipid levels(mmol/L)
ND
HFD
TC
TG
LDL
ns
(F)
HFD
ND
ND-NC
ND-miR-548ag
(G)
Average tumor volume (mm3)
HFD
ND
NC
miR-548ag
(H)
Average tumor weight (g)
HFD
ND
NC
miR-548ag
(I)
Relative expression of miR-548ag
ND
HFD
(J)
CCND1
MOB1B
β-actin
ND
HFD
(K)
Relative expression of miR-548ag
NC
miR-548ag
(L)
CCND1
MOB1B
β-actin
NC
miR-548ag
(M)
Obesity
miR-548ag
MOB1B
YAP1
P
YAP1
CCND1
XIAP
YAP1
EC Cell
cytoplasm
Cell proliferation, anti-apoptosis
nucleus

FIGURE 5 A high-fat diet can promote the expression of miR-548ag, inhibit the expression of MOB1B, and enhance the tumor-forming ability of endometrial cancer (EC) cells. (A) Flow chart of the nude mice experiment ($n = 5$ for each group). (B) General picture of nude mice. (C) Change in body weights of nude mice. (D) Weights of adipose tissue. (E) Blood lipid level. (F) General photograph of tumor tissues. (G) Mean tumor volume. (H) Mean tumor weight. (I) Expression levels of miR-548ag in tumor tissues of mice in the normal-diet group and high-fat diet group. (J) Protein expression levels of MOB1B and CCND1 in tumor tissues of the normal-diet group and high-fat diet group. (K) Expression levels of miR-548ag in tumor tissues of the miR-548ag control group and miR-548ag-overexpression group. (L) Protein expression levels of MOB1B and CCND1 in the miR-548ag control group and miR-548ag-overexpression group. (M) Schematic representation of the role of the MOB1B/YAP1/CCND1/XIAP signaling pathway in promoting the obesity-related progression of EC. *T*-test, Mann–Whitney test, $^{*}p < 0.05$, $^{**}p < 0.01$, $^{***}p < 0.001$.

upregulation of MOB1B reversed the carcinogenic effects of miR-548ag. Although no significant correlation was observed between the mRNA expression of miR-548ag and MOB1B in endometrial tissue, further investigation on a larger patient cohort is required to confirm a correlation. An obese nude mouse model of EC was established to further investigate the function of miR-548ag in EC in vivo. An HFD can promote the expression of miR-548ag and the overexpression of miR-548ag significantly promotes the growth of tumor xenograft, leading to an increased tumor volume. The western blot assay confirmed that the tumors formed by cells transfected with miR-548ag or in the HFD group showed lower levels of MOB1B expression. In summary, miR-548ag possibly represses the expression of tumor suppressor genes such as MOB1B, thus acting as an "oncomir," and indirectly promoting the transcription of genes related to tumorigenesis (Figure 5M).

As mentioned above, a previous study by our group demonstrated that miR-548ag was highly expressed in the sera of obese individuals. This study further confirmed that miR-548ag was also highly expressed in the sera of obesity-related EC patients, although the reasons for this trend need further study. Obesity is a chronic inflammatory state that can cause the release of inflammatory factors and endoplasmic reticulum stress.[25] A study by Sun reported that IL-6 and other inflammatory factors affected the expression and release of microRNAs.[26] The results of a study by Belmont also confirmed that the expression of miRNAs depended on the regulation of endoplasmic reticulum stress.[27] Another study by Yong reported that an increase in the level of palmitic acid and the pro-inflammatory factor TNFα following obesity can promote the expression of miR-34a in the adipose tissue, which is a synergistic effect of the signaling cascade pathways induced by multiple metabolic stresses.[28] However, further investigation is required to confirm whether this causes the increase in the content of miR-548ag in the serum following obesity.

The clinical symptoms of EC are lower abdominal pain, irregular vaginal bleeding, and fluid discharge. At present, the effective treatment methods are mainly the whole uterus, double adnexal and lymphadenectomy, combined with postoperative treatment such as brachyluminal radiotherapy or external pelvic radiotherapy, or chemotherapy based on a pathological report of whether there are high-risk factors.[29] Although early diagnosis, surgery, and chemoradiotherapy have improved treatment outcomes in patients with EC, there is still limited treatment for patients with early disease, the need to preserve fertility, and patients with advanced and recurrent EC, so there is an urgent need to find more effective molecular markers and therapeutic targets.[30] As more and more evidence shows that miRNA is a promising marker for liquid biopsies,[31] miR-548ag can be used for the early diagnosis of obesity-related EC. In conclusion, we demonstrated that highly expressed miR-548ag promoted the occurrence and development of obesity-related EC by inhibiting the MOB1B/YAP1/CCND1/XIAP signaling pathway, which may serve as potential biomarkers and targets for EC diagnosis and treatment.

ACKNOWLEDGMENTS

This research was funded by the Natural Science Foundation of China (82160496) and the Projects of Shihezi University (GJHZ201703).

CONFLICT OF INTEREST

The authors declare no competing interests. All EC patients and non-cancer individuals recruited in the study provided written informed consent.

ETHICS STATEMENT

The study protocol conformed to the ethical guidelines of the Helsinki Declaration and was approved by the First Affiliated Hospital of Shihezi University School Ethics Committee (approval number: 2017-050-01). All procedures involving animals in our study were approved by the First Affiliated Hospital of Shihezi University School Ethics Committee (approval number: A2021-022-01).

ORCID

Jun Zhang https://orcid.org/0000-0001-9796-994X

REFERENCES

1. Sung H, Ferlay J, Siegel RL, et al. Global cancer statistics 2020: GLOBOCAN estimates of incidence and mortality worldwide for 36 cancers in 185 countries. *CA Cancer J Clin*. 2021;71:209-249.
2. Gómez-Raposo C, Merino Salvador M, Aguayo Zamora C, García de Santiago B, Casado Sáenz E. Immune checkpoint inhibitors in endometrial cancer. *Crit Rev Oncol Hematol*. 2021;161:103306.
3. Knez J, Al Mahdawi L, Takač I, Sobočan M. The perspectives of fertility preservation in women with endometrial cancer. *Cancers (Basel)*. 2021;13(4):602.
4. Sung H, Siegel RL, Torre LA, et al. Global patterns in excess body weight and the associated cancer burden. *CA Cancer J Clin*. 2019;69(2):88-112.
5. Onstad MA, Schmandt RE, Lu KH. Addressing the role of obesity in endometrial cancer risk, prevention, and treatment. *J Clin Oncol*. 2016;34(35):4225-4230.
6. Morice P, Leary A, Creutzberg C, Abu-Rustum N, Darai E. Endometrial cancer. *Lancet*. 2016;387(10023):1094-1108.

7. Thomou T, Mori MA, Dreyfuss JM, et al. Adipose-derived circulating miRNAs regulate gene expression in other tissues. *Nature*. 2017;542(7642):450-455.
8. Bartel DP. MicroRNAs: target recognition and regulatory functions. *Cell*. 2009;136:215-233.
9. Rupaimoole R, Slack FJ. MicroRNA therapeutics: towards a new era for the management of cancer and other diseases. *Nat Rev Drug Discov*. 2017;16(3):203-222.
10. Chen S, Sun KX, Liu BL, Zong ZH, Zhao Y. MicroRNA-505 functions as a tumor suppressor in endometrial cancer by targeting TGF-alpha. *Mol Cancer*. 2016;15:11.
11. Agarwal V, Bell GW, Nam J, Bartel DP. Predicting effective microRNA target sites in mammalian mRNAs. *eLife*. 2015;4:e05005.
12. Chen Y, Wang X. miRDB: an online database for prediction of functional microRNA targets. *Nucleic Acids Res*. 2020;48(D1):D127-D131.
13. Lanczky A, Gyorffy B. Web-based survival analysis tool tailored for medical research (KMplot): development and implementation. *J Med Internet Res*. 2021;23(7):e27633.
14. Anaya J. OncoLnc: linking TCGA survival data to mRNAs, miRNAs, and lncRNAs. *PeerJ Comput Sci*. 2016;2:e67.
15. Li JH, Liu S, Zhou H, Qu LH, Yang JH. starBase v2.0: decoding miRNA-ceRNA, miRNA-ncRNA and protein-RNA interaction networks from large-scale CLIP-Seq data. *Nucleic Acids Res*. 2014;42(Database issue):D92-D97.
16. Shi Z, Zhou Q, Gao S, et al. Silibinin inhibits endometrial carcinoma via blocking pathways of STAT3 activation and SREBP1-mediated lipid accumulation. *Life Sci*. 2019;217:70-80.
17. Byrne FL, Poon IKH, Modesitt SC, et al. Metabolic vulnerabilities in endometrial cancer. *Cancer Res*. 2014;74(20):5832-5845.
18. Polusani SR, Huang YW, Huang G, et al. Adipokines deregulate cellular communication via epigenetic repression of gap junction loci in obese endometrial cancer. *Cancer Res*. 2019;79(1):196-208.
19. Rodriguez AC, Vahrenkamp JM, Berrett KC, et al. ETV4 is necessary for estrogen signaling and growth in endometrial cancer cells. *Cancer Res*. 2020;80:1234-1245.
20. Delangle R, De Foucher T, Larsen AK, et al. The use of microRNAs in the Management of Endometrial Cancer: a meta-analysis. *Cancers (Basel)*. 2019;11(6):832.
21. Dogan H, Shu J, Hakguder Z, Xu Z, Cui J. Elucidation of molecular links between obesity and cancer through microRNA regulation. *BMC Med Genomics*. 2020;13(1):161.
22. Fan S, Price T, Huang W, et al. PINK1-dependent mitophagy regulates the migration and homing of multiple myeloma cells via the MOB1B-mediated hippo-YAP/TAZ pathway. *Adv Sci (Weinh)*. 2020;7(5):1900860.
23. Nishio M, Sugimachi K, Goto H, et al. Dysregulated YAP1/TAZ and TGF-β signaling mediate hepatocarcinogenesis in Mob1a/1b-deficient mice. *Proc Natl Acad Sci USA*. 2016;113(1):E71-E80.
24. Quan M, Chen Z, Jiao F, et al. Lysine demethylase 2 (KDM2B) regulates hippo pathway via MOB1 to promote pancreatic ductal adenocarcinoma (PDAC) progression. *J Exp Clin Cancer Res*. 2020;39(1):13.
25. Arner P, Kulyté A. MicroRNA regulatory networks in human adipose tissue and obesity. *Nat Rev Endocrinol*. 2015;11(5):276-288.
26. Sun J, Fu L. IL-6 promotes gastric cancer cell proliferation and EMT through regulating miR-152/PIK3R3 pathway. *Zhong nan Da Xue Xue Bao Yi Xue Ban*. 2017;42(11):1241-1247.
27. Belmont PJ, Chen WJ, Thuerauf DJ, Glembotski CC. Regulation of microRNA expression in the heart by the ATF6 branch of the ER stress response. *J Mol Cell Cardiol*. 2012;52(5):1176-1182.
28. Pan Y, Hui X, Hoo RLC, et al. Adipocyte-secreted exosomal microRNA-34a inhibits M2 macrophage polarization to promote obesity-induced adipose inflammation. *J Clin Invest*. 2019;129(2):834-849.
29. Abu-Rustum NR, Yashar CM, Bean S, et al. Uterine neoplasms, version 3.2019 [EB/OL]. https://www.nccn.org/professionals/physician_gls/default.aspx. Accessed September 16, 2019.
30. Liu Y, Zhao R, Chi S, et al. UBE2C is upregulated by estrogen and promotes epithelial-mesenchymal transition via p53 in endometrial cancer. *Mol Cancer Res*. 2020;18(2):204-215.
31. Valihrach L, Androvic P, Kubista M. Circulating miRNA analysis for cancer diagnostics and therapy. *Mol Aspects Med*. 2020;72:100825.

SUPPORTING INFORMATION

Additional supporting information can be found online in the Supporting Information section at the end of this article.

How to cite this article: Pang H, Wang J, Wei Q, et al. miR-548ag functions as an oncogene by suppressing MOB1B in the development of obesity-related endometrial cancer. *Cancer Sci*. 2023;114:1507-1518. doi:10.1111/cas.15679